HAL
open science

Resolved discrepancies between visible spontaneous Raman cross-section and direct near-infrared Raman gain measurements in TeO2-based glasses

Clara Rivero, Robert Stegeman, Michel Couzi, David Talaga, Thierry Cardinal, Kathleen Richardson, George Stegeman

To cite this version:

Clara Rivero, Robert Stegeman, Michel Couzi, David Talaga, Thierry Cardinal, et al.. Resolved discrepancies between visible spontaneous Raman cross-section and direct near-infrared Raman gain measurements in TeO2-based glasses. Optics Express, 2005, 13 (12), pp.4759-4769. 10.1364/OPEX.13.004759 . hal-00019294

HAL Id: hal-00019294

https://hal.science/hal-00019294v1

Submitted on 13 Feb 2024

HAL is a multi-disciplinary open access archive for the deposit and dissemination of scientific research documents, whether they are published or not. The documents may come from teaching and research institutions in France or abroad, or from public or private research centers.

L'archive ouverte pluridisciplinaire **HAL**, est destinée au dépôt et à la diffusion de documents scientifiques de niveau recherche, publiés ou non, émanant des établissements d'enseignement et de recherche français ou étrangers, des laboratoires publics ou privés.

Resolved discrepancies between visible spontaneous Raman cross-section and direct near-infrared Raman gain measurements in TeO_2-based glasses

Clara Rivero[1,2], Robert Stegeman[1], Michel Couzi[3], David Talaga[3], Thierry Cardinal[2], Kathleen Richardson[1,4], and George Stegeman[1]

[1] College of Optics & Photonics/CREOL, University of Central Florida
4000 Central Florida Blvd., Orlando, FL 32816-2700
[2] Institut de Chimie de la Matiere Condensee de Bordeaux
87 Avenue du Dr. Albert Schweitzer, 33608 Pessac cedex, France
[3] Laboratoire de Physico-Chimie Moleculaire, University of Bordeaux 1
Bât. A12, 33405 Talence cedex, France
[4] School of Material Science and Engineering, Clemson University
161 Sirrine Hall, Box 340971, Clemson, SC 29634-0971
crivero@mail.ucf.edu

Abstract: Disagreements on the Raman gain response of different tellurite-based glasses, measured at different wavelengths, have been recently reported in the literature. In order to resolve this controversy, a multi-wavelength Raman cross-section experiment was conducted on two different TeO_2-based glass samples. The estimated Raman gain response of the material shows good agreement with the directly-measured Raman gain data at 1064 nm, after correction for the dispersion and wavelength-dependence of the Raman gain process.

© 2005 Optical Society of America

OCIS codes: (190.5650) Raman effect; (160.4330) Nonlinear optical materials; (190.5890) Scattering, stimulated; (060.2320) Fiber optics amplifiers and oscillators

References and links

1. M.N. Islam, "Raman Amplifiers for Telecommunications," IEEE J. Sel. Top. Quantum Electron. **8**, 548-559 (2002)
2. M.N. Islam, "*Raman Amplifiers for Telecommunications 1," Physical Principles* (Springer 2004)
3. H.S. Seo and K. Oh, "Optimization of silica fiber Raman amplifier using the Raman frequency modeling for an arbitrary GeO_2 concentration," Opt. Commun. **181**, 145-151 (2000)
4. J. Bromage, K. Rottwitt, and M.E. Lines, "A Method to Predict the Raman Gain Spectra of Germanosilicate Fibers With Arbitrary Index Profiles," Photon. Technol. Lett. **14**, 24-26 (2002)
5. M. E. Lines, "Raman gain estimates for high-gain optical fibers," J. Appl. Phys. **62**, 4363-4370 (1987)
6. M.E. Lines, "Absolute Raman Intensities in Glasses, I. Theory", J. Non-Cryst. Sols. **89**, 143-162 (1987)
7. A. E. Miller, K. Nassau, K. B. Lyons, and M. E. Lines, "The intensity of Raman scattering in glasses containing heavy metal oxides," J. Non-Cryst. Sols. **99**, 289-307 (1988)
8. F.L Galeener, J. C. Mikkelsen Jr., R. H. Geils, and W. J. Mosby, "The relative Raman cross sections of vitreous SiO_2, GeO_2, B_2O_3, and P_2O_5," Appl. Phys. Lett. **32,** 34-36 (1978)
9. R. H. Stolen, "Issues in Raman gain measurements," in Tech. Dig. Symp. Optical Fiber Measurements, NIST Special Publication 953 (National Institute of Standards and Technology), (Gaithersburg, MD, 2000) pp. 139
10. A. Mori, H. Masuda, K. Shikano, K. Oikawa, K. Kato, and M. Shimizu, "Ultra-wideband tellurite-based Raman fibre amplifier," Electron. Lett. **37**, 1442-1443 (2001)

#7468 - $15.00 USD Received 16 May 2005; revised 6 June 2005; accepted 7 June 2005

11. R. Stegeman, L. Jankovic, H. Kim, C. Rivero, G. Stegeman, K. Richardson, P. Delfyett, Y. Guo, A. Schulte, and T. Cardinal, "Tellurite glasses with peak absolute Raman gain coefficients up to 30 times that of fused silica," Opt. Lett. **28**, 1126-1128 (2003)
12. C. Rivero, K. Richardson, R. Stegeman, G. Stegeman, T. Cardinal, E. Fargin, M. Couzi, and V. Rodriguez, "Quantifying Raman Gain Coefficients in Tellurite Glasses," J. Non-Cryst. Sols. **345&346**, 396-401 (2004)
13. R. Stegeman, C. Rivero, K. Richardson, G. Stegeman, P. Delfyett, Y. Guo, A. Pope, A. Schulte, T. Cardinal, P. Thomas, and J-C. Champarnaud-Mesjard, "Raman gain measurements of thallium-tellurium oxide glasses," Opt. Express **13**, 1144-1149 (2005)
14. G. Dai, F. Tassone, A. Li Bassi, V. Russo, C.E. Bottani, and F. D'Amore, "TeO_2-based glasses containing Nb_2O_5, TiO_2, and WO_3 for discrete Raman fiber amplification," Photon. Technol. Lett. **16**, 1011-1013, (2004)
15. G.S. Murugan, T. Suzuki, and Y. Ohishi, "Tellurite glasses for ultrabroadband fiber Raman amplifiers," Appl. Phys. Lett. **86**, 161109 (2005)
16. V. G. Plotnichenko, V. O. Sokolov, V. V. Koltashev, E. M. Dianov, I. A. Grishin, and M. F. Churbanov, "Raman band intensities of tellurite glasses," Opt. Lett. **30**, 1156-1158 (2005)
17. N.L. Boling, A.J. Glass, and A. Owyoung, "Empirical Relationships for Predicting Nonlinear Refractive Index Changes in Optical Solids," IEEE J. Quantum Electron. **14**, 601-608 (1978)
18. F. Yoshino, S. Polyakov, G.I. Stegeman, and M. Liu, "Nonlinear Refraction and Absorption from 1300 to 2200 nm in Single Crystal Polymer poly [bis (p-toluene sulfonate)] of 2, 4-hexadiyne-1, 6-diol (PTS)," Quantum Electronics and Laser Science QELS Prostconference Digest, QTuG43 (2003)
19. V.A. Lisinetskii, I.I. Mishkel, R.V. Chulkov, A.S. Grabtchikov, P.A. Apanasevich, H.J. Eichler, and V.A. Orlovich, "Raman gain coefficient of Barium Nitrate measured for the spectral region of Ti:Sapphire Laser," J. of Nonlinear Opt. Phys. Mat. **14**, 107-114 (2005)
20. Y. Kato and H. Takuma, "Experimental Study on the Wavelength Dependence of the Raman Scattering Cross Sections," J. Chemical Phys. **54**, 5398-5402 (1971)
21. Y. Kato and H. Takuma, "Absolute Measurement of Raman-Scattering Cross Sections in Liquids," J. Opt. Soc. Am. **61**, 347-350 (1971)
22. B. Jeansannetas, S. Blanchandin, P. Thomas, P. Marchet, J. C. Champarnaud-Mesjard, T. Merle-Mejean, B. Frit, V. Nazabal, E. Fargin, G. Le Flem, M. O. Martin, B. Bosquet, L. Canioni, S. Le Boiteux, P. Segonds, and L. Sarger, "Glass structure and optical nonlinearities in thallium(I) tellurium (IV) oxide glasses," J. Sol. St. Chem. **146**, 329 (1999)
23. A. Berthereau, E. Fargin, A. Villezusanne, R. Olazcuaga, G. Le Flem, L.Ducasse, "Determination of local geometries around tellurium in TeO_2-Nb_2O_5 and TeO_2-Al_2O_3 oxide glasses by XANES and EXAFS: investigation of electronic properties of evidenced oxygen clusters by *ab initio* calculations," J. Sol. St. Chem. **126**, 143-151 (1996)
24. M.E. Lines, "Influence of d orbitals on the nonlinear optical response of transparent transition-metal oxides," Phys. Rev. B **43**, 11978-11990 (1991)
25. T. Sekiya, N. Mochida, A. Ohtsuka, and M. Tonokawa, "Raman spectra of $MO_{1/2}$-TeO_2 (M=Li, Na, K, Rb, Cs, and Tl) glasses," J. Non-Cryst. Sols. **144**, 128 (1992)
26. R. H. Stolen and E. P. Ippen, "Raman gain in glass optical waveguides," Appl. Phys. Lett. **22**, 276-273 (1972)
27. R. Stegeman, C. Rivero, G. Stegeman, K. Richardson, P. Delfyett, L. Jankovic, and H. Kim, "Raman gain measurements in bulk glass samples", J. Opt. Soc. Am. B (to be published)
28. F.A. Oguama, H. Garcia, and A.M. Johnson, "Simultaneous measurement of the Raman gain coefficient and the nonlinear refractive index of optical fibers: theory and experiment," J. Opt. Soc. Am. B **22**, 426-436 (2005)
29. M.E. Lines, "Oxide glasses for fast photonic switching: A comparative study," J. Appl. Phys. **69**, 6876-6884 (1991)

1. Introduction

Recent advances in the telecom fiber industry have revived interest in broadband signal amplification, driven by the urgent need for additional bandwidth to satisfy the demands for data transmission, both for long haul and local area networks. Raman amplification has become the preferred approach because it is only restricted by the pump wavelength and the Raman-active modes of the gain medium [1,2]. Currently, fused-silica and germanium-doped silica fibers are the main Raman gain materials used in the telecom industry; however, these fibers have very low Raman gain response, and a limited usable spectral bandwidth of around

#7468 - $15.00 USD Received 16 May 2005; revised 6 June 2005; accepted 7 June 2005
(C) 2005 OSA

5 THz, for single pump excitation [3,4]. This has led to research focused on new Raman gain materials, typically multi-component glasses in the search for compositions to enhance either Raman gain coefficients, or bandwidth, or both.

Since the pioneering work of Lines and colleagues, spontaneous Raman scattering has been the technique of choice for rapid characterization of the wavelength dispersion and magnitude of the Raman gain coefficient [5-7]. Because of its wide acceptance in the fiber industry, the Raman spectrum is typically ratioed to that of fused silica in order to estimate the maximum Raman gain available at the pump laser wavelength for Raman scattering [7,8]. This result is then extrapolated to the communications wavelengths using the known wavelength dispersion in refractive index, as suggested by Stolen [2,9]. This is the currently accepted practice.

Recent publications have identified tellurite-based glasses as promising candidate materials for high Raman amplification applications, due to their high gain coefficients [10-16]. However, discrepancies of up to a factor of two have been reported for Raman gain measured by spontaneous Raman scattering in the visible and direct measurements of the Raman gain coefficient with 1064 nm pumping, even after the usual wavelength dependencies are applied [11,14-16]. In this paper we show that these discrepancies are a direct consequence of wavelength dispersion in the Raman susceptibility itself which is accentuated when the wavelength of the absorption edge of the test glasses occurs near the laser wavelength used for the Raman scattering measurement. Specifically, we demonstrate this by measuring the Raman spectrum, relative to silica, at four wavelengths spanning the range 458 – 1064 nm. Furthermore we also show that in the multi-component glasses the spectrum actually changes its shape with laser wavelength because different Raman vibrations are coupled to different electronic molecular resonances whose peak absorptions occur at different wavelengths.

2. Theoretical background

Frequency dispersion in nonlinear coefficients, including the Raman susceptibility, is well-known in nonlinear optics [17-20]. For the case of Raman scattering, consider a multi-component glass, like the tellurites, with each component having its own distinct vibrational modes and electronic states (labeled by "*r*"). The polarizability of species "*k*" in its own frame of reference, when modulated by its β'th Raman active phonon of amplitude Q_β^k can be written as

$$\alpha_{ij}^k = \sum_r \alpha_{ij}^{k,r}(\omega_1 - \omega_{k,r}) + \sum_r \sum_\beta \{ \frac{\partial \alpha_{ij}^{k,r}(\omega_1 - \omega_{k,r})}{\partial Q_\beta^k} |_{Q_\beta^k = 0} \} Q_\beta^k \tag{1}$$

where $\partial \alpha_{ij}^{k,r}(\omega_1 - \omega_{k,r}) / \partial Q_\beta^k$ is the Raman molecular susceptibility, and ω_1 is the laser excitation (pump) frequency. Note that each contribution to the linear polarizability (first summation in Eqn.1), and the Raman susceptibility (second summation) is associated with an electronic transition in the species centered (in the absorption spectrum) at the frequency $\omega_{k,r}$ with some complex spectral distribution and transition matrix element. From Eqn. 1 the refractive index of the material is given by

$$n^2 = 1 + \frac{1}{\varepsilon_0} \sum_k N_k \Re eal\{ \sum_r \alpha_{ij}^{k,r}(\omega_1 - \omega_{k,r}) \}, \tag{2}$$

where N_k is the number density of species *k* in the glass. (The absorption spectrum is given by the imaginary component). Hence the wavelength dispersion in the refractive index is a

#7468 - $15.00 USD Received 16 May 2005; revised 6 June 2005; accepted 7 June 2005
(C) 2005 OSA

summation of the dispersion due to all of the electronic transitions in all the component species.

Taking into account at the air-glass boundary the Fresnel transmission coefficient and the effect of refraction on the solid angle subtended at the detector for a typical Raman scattering experiment, the ratio of the peak intensity of a Raman scattered line $I_{\beta}^{k,r}(\omega_1 - \Omega_{\beta}^{k})$ in air (at the detector) due to the β'th normal mode of the k'th species to the incident intensity $I_{in}(\omega_1)$ in air, at frequency ω_1 is given by [7,8,21]

$$\frac{I_{\beta}^{k,r}(\omega_1 - \Omega_{\beta}^{k})}{I_{inc}(\omega_1)\Delta\Omega} = K_{SR}^{k,r}(\omega_1 - \Omega_{\beta}^{k})^4 \frac{[1-R(\omega_1)][1-R(\omega_1 - \Omega_{\beta}^{k})]}{[n(\omega_1 - \Omega_{\beta}^{k})]^2} \left| \frac{\partial \alpha_{ij}^{k,r}(\omega_1 - \omega_{k,r})}{\partial Q_{\beta}^{k}} \right|^2 \tag{3}$$

where $\Delta\Omega$ is the solid angle, Ω_{β}^{k} is the frequency shift of the Raman peak from the laser frequency, R is the reflectance coefficient $\left(R(\omega) = \frac{[n(\omega)-1]^2}{[n(\omega)+1]^2} \right)$ at normal incidence, and the $[n(\omega_1 - \Omega_{\beta})]^2$ in the denominator is a consequence of the solid angle correction. Here all of the explicit dependence on frequency has been shown in Eqn. 3 and all of the phonon and electromagnetic parameters, including the Bose-Einstein thermal population factor, are contained in the constant $K_{SR}^{k,r}$. For completeness, the dependence of the Raman gain coefficient (defined for the pump intensity) on frequency is given by

$$\gamma_{\beta}^{k,r}(\omega_1 - \Omega_{\beta}^{k}) = K_{RG}^{k,r} \frac{(\omega_1 - \Omega_{\beta}^{r})}{n(\omega_1 - \Omega_{\beta}^{r})n(\omega_1)} \left| \frac{\partial \alpha_{ij}^{k,r}(\omega_1 - \omega_{k,r})}{\partial Q_{\beta}^{k}} \right|^2, \tag{4}$$

where $K_{RG}^{k,r}$ is a constant that contains all the phonon and electromagnetic constant parameters and is different from $K_{SR}^{k,r}$. When all of the experimental details are taken into account, it is therefore possible to evaluate the Raman gain coefficient from the spontaneous Raman spectrum, at the *same excitation frequency*. The detailed relationship is

$$\gamma_{\beta}^{k,r}(\omega_1 - \Omega_{\beta}^{r}) = \frac{K_{RG}^{k,r}}{K_{SR}^{k,r}} \frac{n(\omega_1 - \Omega_{\beta}^{r})}{(\omega_1 - \Omega_{\beta}^{r})^3 n(\omega_1)[1-R(\omega_1)][1-R(\omega_1 - \Omega_{\beta}^{r})]} \frac{I_{\beta}^{k,r}(\omega_1 - \Omega_{\beta}^{r})}{I_{inc}(\omega_1)\Delta\Omega}. \tag{5}$$

Although the Raman susceptibility also exhibits dispersion with frequency, it is not *á priori* the same as the refractive index dispersion because not all of the vibrational modes couple (modulate) equally to the molecular polarizability [20]. If there is one dominant peak in the Raman spectrum due to coupling to a dominant electronic transition (responsible for the dispersion in the refractive index in the wavelength range of interest), then, assuming that the resonant enhancement in the susceptibility $\partial \alpha_{ij}^{k,r}(\omega_1 - \omega_{k,r}) / \partial Q_{\beta}^{k}$ for frequencies below the band edge is linearly proportional to the resonant enhancement in $\alpha_{ij}^{k,r}(\omega_1 - \omega_{k,r})$,

#7468 - $15.00 USD Received 16 May 2005; revised 6 June 2005; accepted 7 June 2005
(C) 2005 OSA

this enhancement is approximated by $\left(n^2(\omega_1)-1\right)$. This correction has been proven to work in the case of fused silica [2,9]. In fact, usually only a limited number of electronic transitions are important, as is well-known from typical absorption spectra. In general, the closer the laser excitation frequency is to $\omega_{k,r}$ the larger the enhancement in the Raman susceptibility and the more intense the particular Raman peaks will be. Furthermore, in such conditions if two different vibrations couple to susceptibilities whose associated absorption maxima have different resonance frequencies ($\omega_{k,r}$), then their relative contributions to a Raman spectrum will change with frequency ω_1. These are the two features which will be examined experimentally here to test the importance of frequency dispersion of the Raman cross-section on measurements of Raman spectra at different frequencies ω_1 and hence the afore-mentioned differences in reported values.

3. Experimental procedure

The spontaneous Raman cross-section measurements were conducted using a micro-Raman setup. Two lines from an Ar^+ laser (458 nm and 514 nm), the 752 nm line from a Kr^+ laser, and the 1064 nm line from a Nd:YAG laser were used as the excitation wavelengths. In all cases, the incoming polarized (V) laser beam was focused onto the front polished surface of the sample via a 100X microscope objective, with a spatial resolution of about 2 μm. A polarizer was used to select the polarization direction (vertical, V or horizontal, H) of the scattered light. A backscattering geometry was used to collect the Raman signal, which was then spectrally analyzed with a spectrometer and a CCD detector, with a typical resolution of about 6 cm^{-1}. The Rayleigh line was reduced with a holographic notch filter. All spectra were normalized to the peak vibration of SiO_2 at 440 cm^{-1}.

4. Results and interpretation

In order to address this problem, a multi-wavelength Raman cross-section experiment was conducted on two different TeO_2-based glass samples. A tellurium-tungsten oxide glass (glass composition 85% TeO_2 – 15% WO_3) was studied since this composition is similar to that previously studied by the different research groups [14-16]. The other composition studied was a tellurium-niobium oxide glass (composition 85% TeO_2 – 10% Nb_2O_5 – 5% MgO). These two glasses were selected for their enhanced third order nonlinearity, and strong Raman scattering cross-section due to TeO_2, which is further enhanced by the presence of d^0-species such as W^{6+} and Nb^{5+} [22-24]. The extrapolated Raman gain coefficient obtained at the peak of the Raman line shows very good agreement with the directly-measured Raman gain data with 1064 nm pumping, after correction for the index dispersion and excitation frequency-dependence of the Raman gain process.

Table 1 shows the sample composition (in mol%) as well as the respective density and linear refractive index values, for the two TeO_2-based glasses chosen for this multi-wavelength Raman cross-section measurement.

Table 1. Physical Properties

Glass Composition	Sample Code	Density ±0.02 (g/cm^3)	Linear Refractive Index n(λ) ± 0.05 532 / 633 / 1064 nm			$\lambda_{cut\text{-}off}$ (nm)
85%TeO_2 – 15%WO_3	W	5.89	2.16	2.14	2.12	450
85%TeO_2 – 10%Nb_2O_5 – 5% MgO	Nb	5.26	2.08	2.07	2.00	410
SiO_2	SiO_2	2.20	1.461	1.457	1.450*	165

* Linear refractive index for SiO_2 was obtained from the Sellmeier dispersion equation

#7468 - $15.00 USD Received 16 May 2005; revised 6 June 2005; accepted 7 June 2005
(C) 2005 OSA

Note that the simple approximation of the dispersion in the Raman susceptibility for W and Nb is 3.67 (3.33) at 532 nm and 3.49 (3.00) at 1064 nm, for $\left(n^2(\omega_1)-1\right)$. The maximum correction in this case is only 23%.

The measured absorption edge of these glasses is shown in Fig. 1. Notice that even though the absorption bandgap is different for the two TeO_2 samples, they both exhibit an absorption tail up to 550 nm.

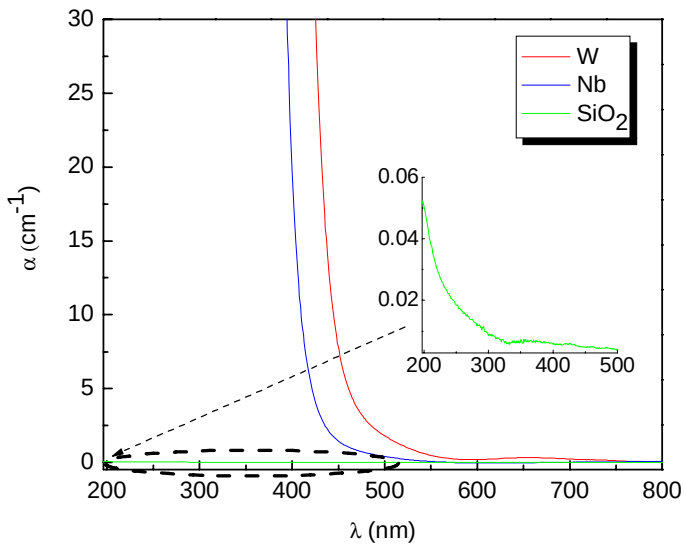

Fig. 1. UV-Vis-NIR absorption spectra of samples W, Nb, and SiO_2. Notice that 195 nm is the lowest wavelength resolution of the Cary500 Spectrophotometer.

Figure 2 illustrates the spontaneous Raman spectra of the two samples, after normalization to SiO_2, as a function of the excitation wavelength. From the preceding discussion on frequency dispersion, the ratio of the Raman gain for a glass at two different frequencies ω_1 and ω_2, is given in terms of the Raman intensities by

$$\frac{\gamma_\beta^{r,k}(\omega_2-\Omega_\beta^r)}{\gamma_\beta^{r,k}(\omega_1-\Omega_\beta^r)}=\frac{(\omega_1-\Omega_\beta^r)^3}{(\omega_2-\Omega_\beta^r)^3}\frac{n(\omega_2-\Omega_\beta^r)n(\omega_1)}{n(\omega_1-\Omega_\beta^r)n(\omega_2)}\frac{\left[1-R(\omega_1-\Omega_\beta^r)\right]\left[1-R(\omega_1)\right]}{\left[1-R(\omega_2-\Omega_\beta^r)\right]\left[1-R(\omega_2)\right]}\times\frac{I_\beta^{k,r}(\omega_2-\Omega_\beta^r)}{I_{inc}(\omega_2)}\frac{I_{inc}(\omega_1)}{I_\beta^{k,r}(\omega_1-\Omega_\beta^r)} \tag{6}$$

Note (1) that these expressions are corrected for internal solid angle, Fresnel transmission and frequency dispersion in the linear index, and (2) that Stolen has found that the ratio for the Raman susceptibility for fused silica is essentially independent of wavelength over the range 526 – 1064 nm (maximum frequency dispersion correction of 5% for this wavelength range) [9]. This is reasonable because the band edge of fused silica occurs at about 165 nm, well-removed from 458 nm (our lowest experimental wavelength). Therefore normalizing the Raman data for the tellurite glasses to that of fused silica reveals the dispersion properties of the Raman susceptibility of those glasses. Furthermore, by measuring the Raman spectra of a test glass under the same experimental conditions as for fused silica at a laser wavelength for

#7468 - $15.00 USD Received 16 May 2005; revised 6 June 2005; accepted 7 June 2005
(C) 2005 OSA

which the peak Raman gain for fused silica is known, the peak Raman gain of the test glass at that frequency for a Raman active mode can be deduced, $\frac{\gamma_{\beta}^{r,k}(\omega_1-\Omega_{\beta}^{r})}{\gamma_{\beta'}^{r',k'}(\omega_1-\Omega_{\beta'}^{r'})}=$

$$\frac{(\omega_1-\Omega_{\beta'}^{r'})^3}{(\omega_1-\Omega_{\beta}^{r})^3}\frac{n(\omega_1-\Omega_{\beta}^{r})n'(\omega_1)}{n'(\omega_1-\Omega_{\beta'}^{r'})n(\omega_1)}\frac{[1-R'(\omega_1-\Omega_{\beta'}^{r'})][1-R'(\omega_1)]}{[1-R(\omega_1-\Omega_{\beta}^{r})][1-R(\omega_1)]}\frac{I_{\beta}^{k,r}(\omega_1-\Omega_{\beta}^{r})}{I_{inc}(\omega_1)}\frac{I_{inc}'(\omega_1)}{I_{\beta'}^{r',k'}(\omega_1-\Omega_{\beta'}^{r'})}$$

where the prime parameters belong to fused silica. Explicitly, $\Omega_{\beta'}^{r'}$ is the peak Raman frequency shift at 440 cm^{-1} ($\Delta\upsilon$ = 13.2 THz) in fused silica, and Ω_{β}^{r} is the Raman active mode of either the 665 cm^{-1} ($\Delta\upsilon$ = 20 THz) or 920 cm^{-1} ($\Delta\upsilon$ = 27.6 THz) vibration in the tellurite glass. The reason for the analysis of both Raman active modes in a tellurite glass with respect to fused silica is discussed later in the text.

Once this value is found for the test glass, the *"almost"* frequency independence of the fused silica Raman susceptibility allows the frequency dependence of the Raman susceptibility of the test glass to be evaluated by ratioing the test glass Raman intensity spectrum to that of fused silica at the new frequency. By normalizing to fused silica, a frequency-independent Raman susceptibility for the glass with respect to fused silica (for the test glass) would be expected to yield a curve with zero slope when $\frac{\gamma_{\beta}^{r,k}\left(\omega_1-\Omega_{\beta}^{r}\right)}{\gamma_{\beta'}^{r',k'}\left(\omega_1-\Omega_{\beta'}^{r'}\right)}$ is plotted as a function of pump wavelength. This is not the case according to Fig. 2.

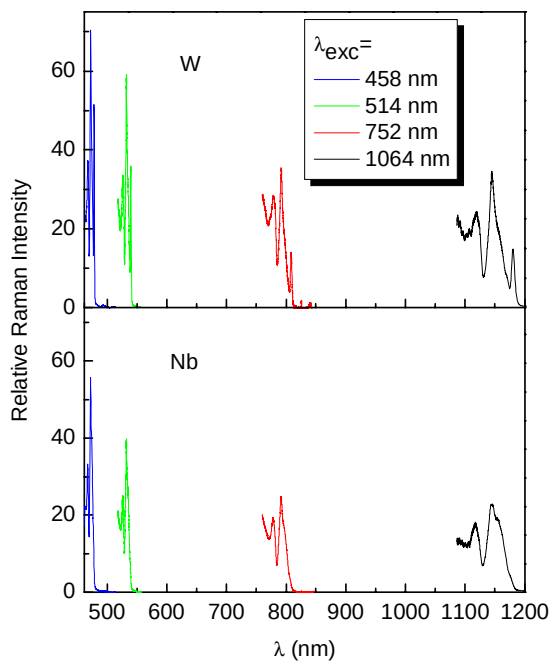

Fig. 2. VV Polarized Experimental Spontaneous Raman Spectrum of samples W and Nb, normalized to SiO_2

#7468 - $15.00 USD
Received 16 May 2005; revised 6 June 2005; accepted 7 June 2005
(C) 2005 OSA

From Fig. 2 a large decrease in the relative intensity of the Raman scattered signal with increasing excitation wavelength between 458 and 752 nm is clear. Note that since all the spectra have been normalized to SiO_2, the $1/\lambda^4$-wavelength dependence cancels out. This result clearly illustrates a strong dispersion dependence of the Raman susceptibility tensor.

It is useful to examine the origin of the Raman peaks observed in the two glasses. Figure 3 shows the VV polarized spontaneous Raman spectra of the two different glasses at 514 nm. The main Raman vibrations in both glasses correspond to the tellurium-oxygen vibrational modes. The main peaks, located at around 450, 665, and 920 cm^{-1} ($\Delta\upsilon$ = 13.5 THz, 20 THz, and 27.6 THz), are attributed to the Te-O-Te chain unit symmetric stretching mode, the TeO_4 bi-pyramidal units, and the isolated W-O short bond vibrations respectively. The shoulders at 750 and 880 cm^{-1} ($\Delta\upsilon$ = 22.5 THz and 26.4 THz) have been assigned to the TeO_{3+1} and/or TeO_3 trigonal pyramids vibrational units, and the Nb-O vibrations, respectively [25].

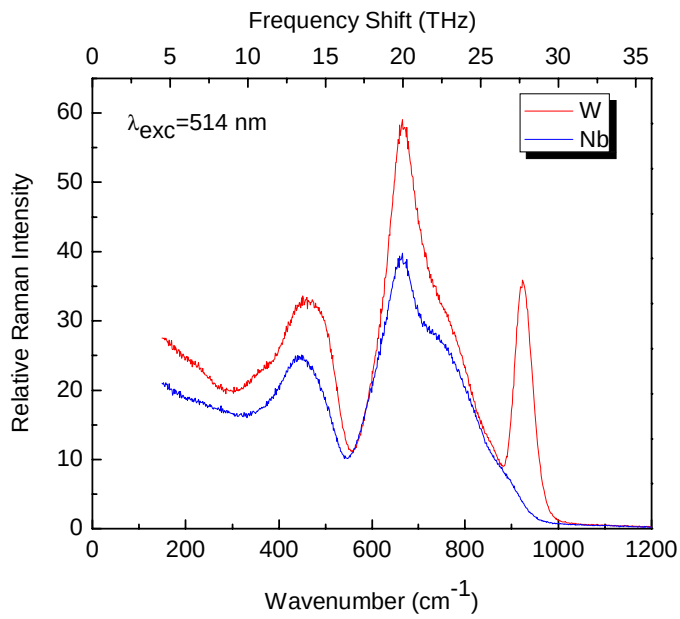

Fig. 3. VV Polarized Spontaneous Raman Spectrum of samples W and Nb, normalized to SiO_2. Excitation wavelength 514 nm

The Raman gain spectra were obtained from the spontaneous Raman cross-section measurements at the different wavelengths. As previously discussed, the Raman gain spectrum parallels the spontaneous Raman cross-section, after correction for the Bose-Einstein correction factor [26], and the Raman gain coefficient can be obtained using Eqn. 6 once a measured value at a specific wavelength is known. The value of the Raman gain of γ = 1.5 ± 0.15 x 10^{-13} m/W (for a frequency shift of 330 cm^{-1} ($\Delta\upsilon$ = 9.9 THz)) as measured by Stolen et. al. with 526 nm pumping was used to fix the value of γ at 514 nm. Figure 4 illustrates the Raman gain coefficient obtained for the strongest Raman resonance in these glasses at 665 cm^{-1} ($\Delta\upsilon$ = 20 THz), attributed to the TeO_4 bi-pyramidal units, and the 920 cm^{-1} vibration attributed to W-O short bond, as discussed above. Also shown in Fig. 4 is the Raman gain obtained by using a crude approximation to the wavelength dispersion in the Raman susceptibility as $\left(n^2(\omega_1 - \Omega^r_\beta) - 1\right)^2$ [2,9].

#7468 - $15.00 USD
Received 16 May 2005; revised 6 June 2005; accepted 7 June 2005
(C) 2005 OSA

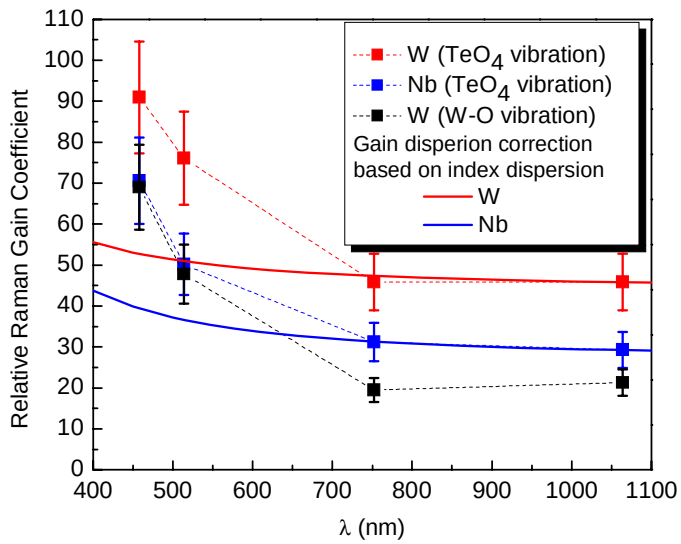

Fig. 4. Estimated multi-wavelength Raman gain coefficient at the peak Raman vibration (TeO_4 units at 665 cm^{-1} ($\Delta\upsilon$ = 20 THz)), and W-O vibration (at 920 cm^{-1} ($\Delta\upsilon$ = 27.6 THz)) respectively, normalized to SiO_2. The dash line is used as a guide to the eye. The solid lines represent the $\left(n^2(\lambda)-1\right)^2$ approximation to the dispersion.

It is clear from Fig. 4, that there is a factor of two discrepancy between the cross-section measurements conducted in the blue-green visible wavelengths, as compared to the cross-section data obtained in the NIR region. There is a resonance enhancement of the Raman cross-section because the spontaneous Raman measurements were conducted near the absorption edge of the material. Hence, this result indicates that the laser wavelength is close to the electronic dipole transition coupled to this particular vibrational mode. Furthermore, in these cases, the crude approximation for the wavelength dependence of the Raman susceptibility strongly underestimates the measured wavelength dependence. Note that for wavelengths longer than 752 nm, the relative gain coefficient is essentially independent of wavelength to within the experimental error.

Direct Raman gain measurements were conducted with 1064 nm pumping on the same samples using the Raman gain setup described in [11,13,27]. Notice that using this technique, one can extract the *absolute* Raman gain coefficient without normalization to any reference standard (pure fused silica is used as a calibration check to ensure the accuracy and precision of the Raman gain measurements made on other materials of interest). Table 2 shows the values of the directly measured Raman gain coefficient of both bulk samples at the 665 cm^{-1} ($\Delta\upsilon$ = 20 THz) Raman resonance, along with the estimated values obtained from the relative cross-section Raman scattering measurements performed with 1064 nm pumping. The values in Table 2 differ from those in [11] because the depolarization ratio defined in [25] was not applied at that time, and it is an additional correction factor that is necessary in the direct Raman gain measurement technique. Note that in order to correct to the absolute Raman gain coefficients, such as those reported in [11], the Raman gain coefficients obtained from the spontaneous Raman spectra, must be multiplied by the Raman gain response of SiO_2 at the 440 cm^{-1} ($\Delta\upsilon$ = 13.2 THz) peak vibration. Typical measured gain coefficients for fused-silica at the 440 cm^{-1} ($\Delta\upsilon$ = 13.2 THz), using a 1064 nm pump excitation, range from 0.92 to 0.74 x

#7468 - $15.00 USD Received 16 May 2005; revised 6 June 2005; accepted 7 June 2005
(C) 2005 OSA

10^{-13} m/W [28]. In this particular paper we use a measured value of $0.89 \pm 0.2 \times 10^{-13}$ m/W with 1064 nm pumping, using the setup described in [11,13,27]. The agreement between the directly measured value and that deduced from the spontaneous Raman measurement for the Raman gain coefficient results verifies the validity and consistency of both techniques. Furthermore, it is clear that the reported discrepancies in Raman gain coefficients between references [14-16] and [11] are due to the resonant enhancement of the Raman susceptibility coefficient in the visible which was not known at that time.

Table 2. Calculated and Experimentally measured Raman Gain coefficient with 1064 nm pumping, at the peak Raman resonance at 665 cm^{-1} ($\Delta\upsilon$ = 20 THz)

Sample Code	Calculated Peak Raman Gain Coefficient at 1064 nm (from Spontaneous Raman cross-section)	Experimentally-obtained Peak Raman Gain Coefficient at 1064 nm
W	40×10^{-13} m/W ± 15%	38×10^{-13} m/W ± 10%
Nb	26×10^{-13} m/W ± 15%	26×10^{-13} m/W ± 10%

Further evidence for the role played by a close proximity of the Raman scattering excitation laser frequency to the frequency associated with the electronic transitions which couple to the vibrations was obtained by studying the *shape* of the Raman spectrum at *different wavelengths*. This can be demonstrated by identifying Raman peaks for which the Raman-relevant electronic transitions are well-separated in frequency, but still close to the laser frequency. Lines has estimated the effective Sellmeier gap E_S(eff) value for single-crystals transition metal (TM) oxides with empty d-bands and TeO_2, and found that the electronic transitions for the species WO_3, Nb_2O_5 and TeO_2 occur at ~ 4.5, 6.8 and 6.3 eV respectively, corresponding to vacuum wavelengths of 276, 183 and 197 nm [24,29]. While the differences in the local environment between single crystals and a multi-component glass would be expected to affect primarily the shape and spectral width of the electronic transitions, it is reasonable to assume that the actual peak transition wavelengths would only be affected weakly. We use these values for $\lambda_{k,r}$ of the dominant transitions responsible for the Raman susceptibility. The dominant vibrational Raman peaks associated with these species occur at 920 cm^{-1}, 880 cm^{-1}, and 665 cm^{-1} ($\Delta\upsilon$ = 27.6 THz, 26.4 THz, and 20 THz) respectively. The Raman peaks at 920 cm^{-1} and 665 cm^{-1} ($\Delta\upsilon$ = 27.6 THz and 20 THz) are strong in the 85%TeO_2 – 15%WO_3 sample and the difference in the wavelengths associated with the electronic transitions is large, 79 nm versus 14 nm for the 85% TeO_2 – 10% Nb_2O_5 – 5% MgO sample respectively. Hence the sample W is the obvious choice for these measurements.

Although both Raman peaks of W are probably resonantly enhanced in the visible, the relative location of the absorption peaks implies that the enhancement should be larger for the 920cm^{-1} ($\Delta\upsilon$ = 27.6 THz) Raman line, as is also evident from Fig. 4. In fact, a large resonance enhancement of the 920 cm^{-1} ($\Delta\upsilon$ = 27.6 THz) Raman vibration was observed for wavelengths in the visible, after normalizing to the peak Raman gain coefficient at 665 cm^{-1} ($\Delta\upsilon$ = 20 THz). This is shown in Fig. 5, along with the Raman gain spectrum obtained by the direct gain measurement technique with 1064 nm pumping. This change in the spectrum fully supports our hypothesis that electronic enhancement occurs in these glasses because the Raman spectrum was measured with laser wavelengths near the absorption edge of the glasses. Furthermore, the spectra obtained from the spontaneous Raman and direct measurement experiments with 1064 nm pumping are in better agreement than the spontaneous Raman spectrum used in [11] since the spontaneous Raman spectrum used in [11] was obtained at 514 nm pumping (the green curve in Fig. 5).

#7468 - $15.00 USD Received 16 May 2005; revised 6 June 2005; accepted 7 June 2005
(C) 2005 OSA

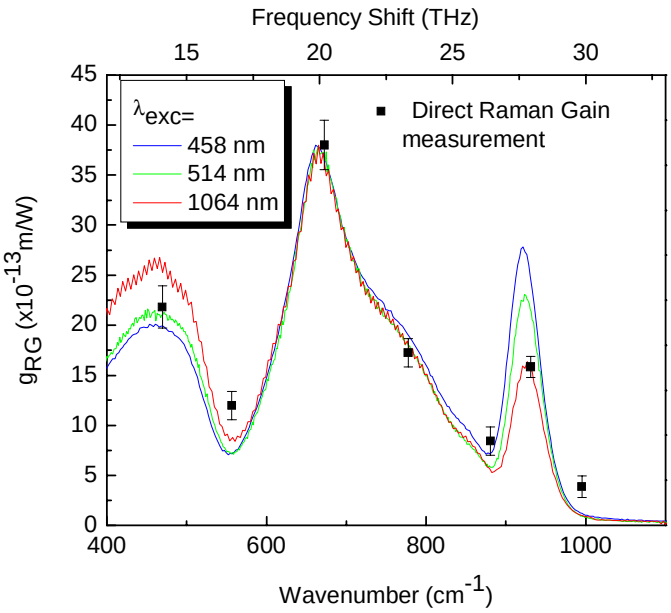

Fig. 5. Spontaneous Raman spectra of 85% TeO_2 – 15% WO_3 obtained at different wavelengths, normalized to the peak Raman gain value at 665 cm^{-1} ($\Delta\upsilon$ = 20 THz), measured with 1064 nm pumping.

5. Conclusion

In conclusion, we have experimentally demonstrated that there is significant dispersion with wavelength in the Raman susceptibility tensor for spontaneous Raman measurements taken near the band edge. Also shown were changes with wavelength in the *shape* of the Raman spectrum of multi-component glasses when measured under these conditions. Thus, even though spontaneous Raman scattering measurement is the preferred tool to measure the Raman gain response of materials, one should consider the appropriate corrections when conversions from measurement to operating wavelengths are needed. Finally, the discrepancies reported in the literature for Raman gain coefficients of tellurites in the visible versus at 1064 nm pumping have been resolved.

Acknowledgments

This work was carried out with the support of a number of research, equipment, and educational grants, including NSF grants ECS-0123484, ECS-0225930, INT-0129235, NSF IGERT grant DGE-0114418, and NSF-CNRS grant 13050. The authors acknowledge the assistance and support of our collaborators at ICMCB / LPCM, and the College of Optics and Photonics / CREOL.